Wigner distribution function for Euclidean systems

Wigner distribution function for Euclidean systems

Luis Miguel Nieto†, Natig M Atakishiyev‡, Sergey M Chumakov§ and Kurt Bernardo Wolf§

† Departamento de Física teórica, Universidad de Valladolid, Spain
‡ Instituto de Matemáticas, UNAM
§ Instituto de Investigaciones en Matemáticas Aplicadas y en Sistemas—Cuernavaca, Universidad Nacional Autónoma de México, Apartado Postal 48–3 62251 Cuernavaca, Morelos, México

Abstract. Euclidean systems include poly- and monochromatic wide-angle optics, acoustics, and also infinite discrete data sets. We use a recently defined Wigner operator and (quasiprobability) distribution function to set up and study the phase-space evolution of these models, subject to differential and difference equations, respectively. Infinite data sets and two-dimensional monochromatic (Helmholtz) fields are thus shown by their Wigner function on a cylinder of (2π) direction and location; the Wigner function for polychromatic wavefields has $\mathbb{R}^3$ 'c-number' coordinates of (two-dimensional) wavenumber and position.

1. Introduction

This section reviews the Wigner operator and function that we introduced [1] to generalize the commonly used Wigner function on phase space. We examine the Newton equation as a starting point for embedding physical models into Lie algebras and present the organization of this paper.

1.1. Definition of the Wigner operator and Wigner function

Consider a Lie group G with N generators X_n, $n = 1, 2, \ldots, N$, in which its elements $g[\gamma]$ are parametrized in *polar* coordinates

$$g[\gamma] = \exp(i\gamma^\top X) = \exp\left(i\sum_{n=1}^{N} \gamma_n X_n\right) \tag{1.1}$$

with γ in a region $R_G \subset \mathbb{R}^N$. The group identity is $g[0]$ and we regard γ as a column vector. Polar parameter arguments will be indicated by brackets.

The *Wigner operator* $\mathcal{W}^G(x)$, of a column vector $x \in \mathbb{R}^N$, is given [2] by

$$\mathcal{W}^G(x) = \int_{R_G} \mathrm{d}g[\gamma] \exp(-i\gamma^\top x)g[\gamma] = \int_{R_G} \mathrm{d}g[\gamma] \exp\left[i\sum_n \gamma_n(X_n - x_n)\right] \tag{1.2}$$

where $\int_{R_G} \mathrm{d}g[\cdots]\gamma$ is the Haar integral with respect to the invariant measure over G.

A physical *model* is introduced by providing a Hilbert space $\mathcal{H} \subset \mathcal{L}^2(G)$ of wavefunctions ϕ, ψ, with inner product $(\phi, \psi)_{\mathcal{H}}$. Here $\mathcal{H}$ is a homogeneous space for

G under unitary right group action $g\psi(h) = \psi(hg)$, and where the real spectra of the self-adjoint generators X_n is endowed with a physical intepretation. We thus build the following sesquilinear functional of $\phi, \psi \in \mathcal{H}$, which is also a function over $x \in \mathbb{R}^N$,

$$W^G(\phi, \psi|x) = (\phi, \mathcal{W}^G(x)\psi)_\mathcal{H} \tag{1.3a}$$

that we have called the *Wigner function* over G. When $\phi = \psi$, as is often used, we shall simply write $W^G(\psi|x)$.

In the case $\mathcal{H} = \mathcal{L}^2(G)$, writing $g' = g[\gamma']$, the Wigner function can be expressed generically as

$$W^G(\phi, \psi|x) = \iint_{R_G} dg[\gamma]\, dg[\gamma']\phi(g'g^{-1/2})^* \exp(-i\gamma^\top x)\psi(g'g^{+1/2}) \tag{1.3b}$$

where in polar coordinates $g^\alpha[\gamma] = g[\alpha\gamma]$. Most models will use homogeneous spaces which are coset spaces of the group, so $\psi(hg) = \psi(g)$ is a function of fewer than the N coordinates (1.1) of the group. Equations (1.3) may be used to find the reduced form of the Wigner function in those cases.

1.2. Covariance

The Wigner operator and function are *covariant*: since the column vector of generators of G in (1.1) transforms as a row vector under the $N \times N$ *adjoint* representation of the group, i.e. by the matrix $\mathbf{D}^{ad}(g)^\top$, the polar coordinates transform as

$$\begin{aligned}
g_0^{-1}g[\gamma]g_0 &= \exp(i\gamma^\top(g_0^{-1}Xg_0)) = \exp(i\gamma^\top\mathbf{D}^{ad}(g_0)^\top X) \\
&= \exp(i(\mathbf{D}^{ad}(g_0)\gamma)^\top X) = g[\mathbf{D}^{ad}(g_0)\gamma].
\end{aligned} \tag{1.4}$$

We regard thus γ as a column vector.

Due to the invariance of the Haar integral $\int_G dg f(g) = \int_G dg\, f(gg_0)$, the Wigner operator (1.2) has the property

$$g_0^{-1}\mathcal{W}^G(x)g_0 = \mathcal{W}^G(\mathbf{D}^{ad}(g_0)x). \tag{1.5}$$

If $\mathcal{T}(g_0)$ is the group representation in the Hilbert space $\mathcal{H}$, then the property of covariance of their Wigner function is

$$W^G(\mathcal{T}(g_0)\phi, \mathcal{T}(g_0)\psi|x) = W^G(\phi, \psi|\mathbf{D}^{ad}(g_0)x). \tag{1.6}$$

This argument also holds true when the group of automorphisms of the Lie algebra of G is larger than G itself. Such are the cases of the Heisenberg–Weyl algebra under linear symplectic transformations, and the Euclidean algebra under SO(2,1) relativistic ones.

1.3. Irreducible representations and Wigner functions

When the function ψ over the homogeneous space $\mathcal{H}$ considered in (1.3a) is decomposed into unitary irreducible representations (unirreps) $\lambda \in \widehat{G}$ (where $\widehat{G}$ is the space of unirreps with Plancherel measure $d\mu(\lambda)$), as $\psi(h) = \int_{\widehat{G}} d\mu(\lambda)\psi_\lambda(h)$, then the Wigner function will decompose accordingly. This is so because the Casimir operator commutes with all $g[\gamma] \in G$, and will thus also commute with the Wigner operator (1.2). Finally, since the inner product over $\mathcal{H}$ in (1.3a) is zero unless both functions belong to the same unirrep λ, it holds that

$$W^G(\phi, \psi|x) = \int_{\widehat{G}} d\mu(\lambda)(\phi_\lambda, \mathcal{W}^G\psi_\lambda)_\mathcal{H} = \int_{\widehat{G}} d\mu(\lambda)W_\lambda^G(\phi_\lambda, \psi_\lambda|x). \tag{1.7}$$

Generally $W_\lambda^G(\phi, \psi | x)$ assumes an analytic and more manageable form because the group action indicated involves well known unirrep matrix elements given in terms of special functions.

1.4. Heisenberg–Weyl and SU(2) systems

In [2] it was shown that when G is the Heisenberg–Weyl group of quantum mechanics (QM), the above construction leads to the commonly known Wigner distribution function [1]

$$W^{\mathrm{QM}}(\phi, \psi | q, p, \hbar) = \frac{1}{2\pi\hbar} \int_{\mathbb{R}} \mathrm{d}x\, \phi\left(q - \frac{1}{2}x\right)^* \mathrm{e}^{-\mathrm{i}xp/\hbar} \psi\left(q + \frac{1}{2}x\right) \quad (1.8)$$

usually written for $\phi = \psi$. In [2] the *three* generators of the Heisenberg–Weyl group were used in the model of polychromatic paraxial optics. There, the reduced *wavelength* $\lambda/2\pi \in \mathbb{R} - \{0\}$ is the spectrum of the central generator (multiplication by $\bar{\lambda}$). In the QM model, nature is constrained to the fixed irreducible representation $\hbar$ of the Heisenberg–Weyl group.

In [3, 4], we examined the group SU(2), whose representations ℓ provided the $(2\ell + 1)$-dimensional homogeneous spaces of finite data sets $\{\psi_m\}_{m=-\ell}^{\ell}$ in a *finite waveguide model*. The physical realization of this model is a multimodal optical waveguide which is capable of carrying only a finite number of modes (a finite oscillator), and whose wavefield is sampled at most at the same number of sensors across the guide.

In the two groups studied, the Wigner function (1.3) depends on three group parameters. Indeed, whereas the common QM Wigner function (1.4) is usually seen as a phase-space construction, our formulation of Wigner functions is endowed with *c*-number arguments equal in number to the parameters of the group.

1.5. Euclidean systems

The purpose of this paper is to build and examine the Wigner function (1.3) for several physical models for which the Euclidean group of rigid motions of the 2-plane serves as a dynamical symmetry group. These systems obey the *free Newton* equation. In this classical equation we replace time derivatives by a Lie bracket with a *Hamiltonian* evolution operator H,

$$\ddot{q} = 0 \implies [H, [H, Q]] = 0. \quad (1.9)$$

The *momentum* operator is, by definition, the Lie bracket of H with the position operator Q, times $-\mathrm{i}$, that is,

$$[H, Q] = -\mathrm{i}P. \quad (1.10)$$

This is the first Hamilton equation, whose content is purely geometrical. Equation (1.9) thus becomes the second Hamilton equation,

$$[H, P] = 0 \quad (1.11)$$

which contains the dynamics of the system. Nothing has been said so far about the Lie bracket $[Q, P]$. If we require that Q, P and H close into a Lie algebra (thus assuring that the system is integrable), the Jacobi identity implies that

$$[H, [Q, P]] = 0. \quad (1.12)$$

Newton's free equation (1.9) is satisfied when $[Q, P]$ commutes with H. QM takes this to be $\hbar\mathbf{1}$ and leads to the familiar free-particle model with $H \sim \frac{1}{2}P^2$. Our choice here is to propose $[Q, P]$ to be a *linear* function of H, and the Lie algebra

$$[Q, P] = -\mathrm{i}H \qquad [Q, H] = \mathrm{i}P \qquad [P, H] = 0. \tag{1.13}$$

This is the Euclidean algebra $e_2 = \mathrm{iso}(2)$ of the Lie group $E_2 = \mathrm{ISO}(2)$. We thus call the systems *Euclidean*. Note that the Wigner function on E_2 can also be used to describe systems whose Hamiltonian belongs to the *enveloping* algebra of E_2.

1.6. Outline

It will serve the scope of this paper to start section 2 with a study of the 'trivial' Lie groups of a single generator. In this case the Wigner function (1.3) is a function of a single variable and the formalism reveals some basic features of our construction. Section 3 collects several elementary results on the three-parameter Euclidean group ISO(2) that will be needed in the rest of the paper.

Two distinct Euclidean optical models are studied: the discrete model in section 4, and the related 2π wave and Helmholtz models in section 5. Discrete two-dimensional optics refers to homogeneous medium where a linear array of sensors samples a monochromatic field; in effect, the Lie algebra includes difference operators and the construction is applicable to general infinite, discrete data sets. 'Gaussian' beams in particular, are examined and plotted for both optical models. We plot the Wigner function of 2π-wavefields on the surface of a cylinder, which plays the role of the natural phase space for Euclidean systems. This allows us to recognize wide-waist or wide-angle Gaussian beams, as well as the interference phenomenon (Moiré pattern) for two such beams in Schrödinger-cat-like wavefields. Finally, section 6 offers some conclusions and directions of research for Wigner functions on other Lie groups.

2. Wigner function on one-parameter groups

We first examine the Wigner operator and Wigner function on one-parameter Lie groups: the group of translations T(1) of the real line $\mathbb{R}$, and the group of rotations SO(2) of the circle $\mathcal{S}_1$. Although apparently trivial, this will evince some basic properties of Wigner functions on the groups whose semidirect product is the Euclidean group, $E_2 = \mathrm{ISO}(2)$.

2.1. One-dimensional translations

The T(1) group elements $g[\gamma] = \exp(\mathrm{i}\gamma Q)$, $\gamma \in \mathbb{R}$, have product law $g[\gamma_1]g[\gamma_2] = g[\gamma_1 + \gamma_2]$, unit element $g(0)$, and inverse $g[\gamma]^{-1} = g[-\gamma]$. The Haar measure is simply $\mathrm{d}\gamma$. The Wigner operator (2.2) on T(1) is

$$\mathcal{W}^{\mathrm{T}(1)}(x) = \int_{\mathbb{R}} \mathrm{d}\gamma\, \mathrm{e}^{-\mathrm{i}x\gamma} g[\gamma] \tag{2.1}$$

with $x \in \mathbb{R}$. In the Hilbert space $\mathcal{L}^2(\mathbb{R})$, the *position* realization is characterized by the single diagonal generator Q, i.e.

$$g[\gamma]\psi(q) = \mathrm{e}^{\mathrm{i}\gamma q}\psi(q) \qquad q \in \mathbb{R}. \tag{2.2}$$

In this case, the Wigner function (2.3) is of a single variable,

$$W^{\mathrm{T}(1)}(\phi, \psi|x) = \int_{\mathbb{R}} \mathrm{d}q\, \phi^*(q) \int_{\mathbb{R}} \mathrm{d}\gamma\, \mathrm{e}^{\mathrm{i}\gamma(q-x)}\psi(q) = 2\pi\phi^*(x)\psi(x). \tag{2.3}$$

In T(1) thus, we have simply $W^{\mathrm{T}(1)}(\psi|x) = 2\pi|\psi(x)|^2$; a real, positive function.

2.2. One-dimensional rotations

In the case of SO(2), where $g[\gamma] \equiv g[\gamma + 2\pi]$, and $\gamma \in (-\pi, \pi]$, the Wigner operator is as (2.1) but with the range of integration over $\mathcal{S}_1$, and the position realization of the group is over the set of *integers* $m \in \mathbb{Z}$, so the Hilbert space of wavefunctions is $\ell^2(\mathbb{Z})$: square-summable sequences on the integers,

$$g[\gamma]\psi_m = \mathrm{e}^{\mathrm{i}\gamma m}\psi_m \qquad m \in \mathbb{Z}. \tag{2.4}$$

The Wigner function (2.3) is thus given by

$$W^{\mathrm{SO}(2)}(\phi, \psi|x) = \sum_{m \in \mathbb{Z}} \phi_m^* \int_{\mathcal{S}_1} \mathrm{d}\gamma \, \mathrm{e}^{\mathrm{i}\gamma(m-x)} \psi_m. \tag{2.5}$$

For x not integer, the integrand in (2.5) is multivalued on the circle; if the integral is taken over $c - \pi < \gamma \leqslant c + \pi$, there will appear a phase factor $\mathrm{e}^{\mathrm{i}c(m-x)}$. To have a real Wigner function for $\phi = \psi$ (below), we should integrate as $\int_{\mathcal{S}_1} = \int_{-\pi}^{\pi}$. Thus (2.5) becomes

$$W^{\mathrm{SO}(2)}(\phi, \psi|x) = 2\pi \sum_{m \in \mathbb{Z}} \phi_m^* \operatorname{sinc}(\pi(m-x))\psi_m \tag{2.6}$$

where $\operatorname{sinc} \rho = \rho^{-1} \sin \rho$ is the *sinus cardinalis* function. We thus see that although the wavefunctions are defined over a discrete set, the Wigner function interpolates its values by the sinc-smoothing common in Fourier wave optics [5]. In figure 1 we show the Wigner function $W^{\mathrm{SO}(2)}(\psi|x)$ of a simple 'signal' $\{\psi_m\}_{m \in \mathbb{Z}}$. Note that there are small intervals (that do not include the integers) where the Wigner function is *negative*; that is why it is called a *quasi*probability distribution function. In this simple SO(2) case, the origin of negativity is simply the behaviour of the interpolating sinc function. At integer points $\operatorname{sinc} \pi(m-x) = \delta_{m,x}$ is a Kronecker delta. The only signal for which the SO(2) Wigner function is everywhere positive is $\psi_m = \text{constant}$.

2.3. Functions on the circle

The only realization of SO(2) with the diagonal generator Q is (2.2), for functions ψ_m on the integers. These are the Fourier series coefficients of functions on the circle. To represent (2.4) in a form involving square-integrable functions on the circle $\phi^\circ, \psi^\circ \in \mathcal{L}^2(\mathcal{S}_1)$, we write

$$\phi_m = \frac{1}{\sqrt{2\pi}} \int_{\mathcal{S}_1} \mathrm{d}\theta \phi^\circ(\theta)\mathrm{e}^{-\mathrm{i}m\theta} \qquad \phi^\circ(\theta) = \frac{1}{\sqrt{2\pi}} \sum_{m \in \mathbb{Z}} \phi_m \mathrm{e}^{\mathrm{i}m\theta} \tag{2.7}$$
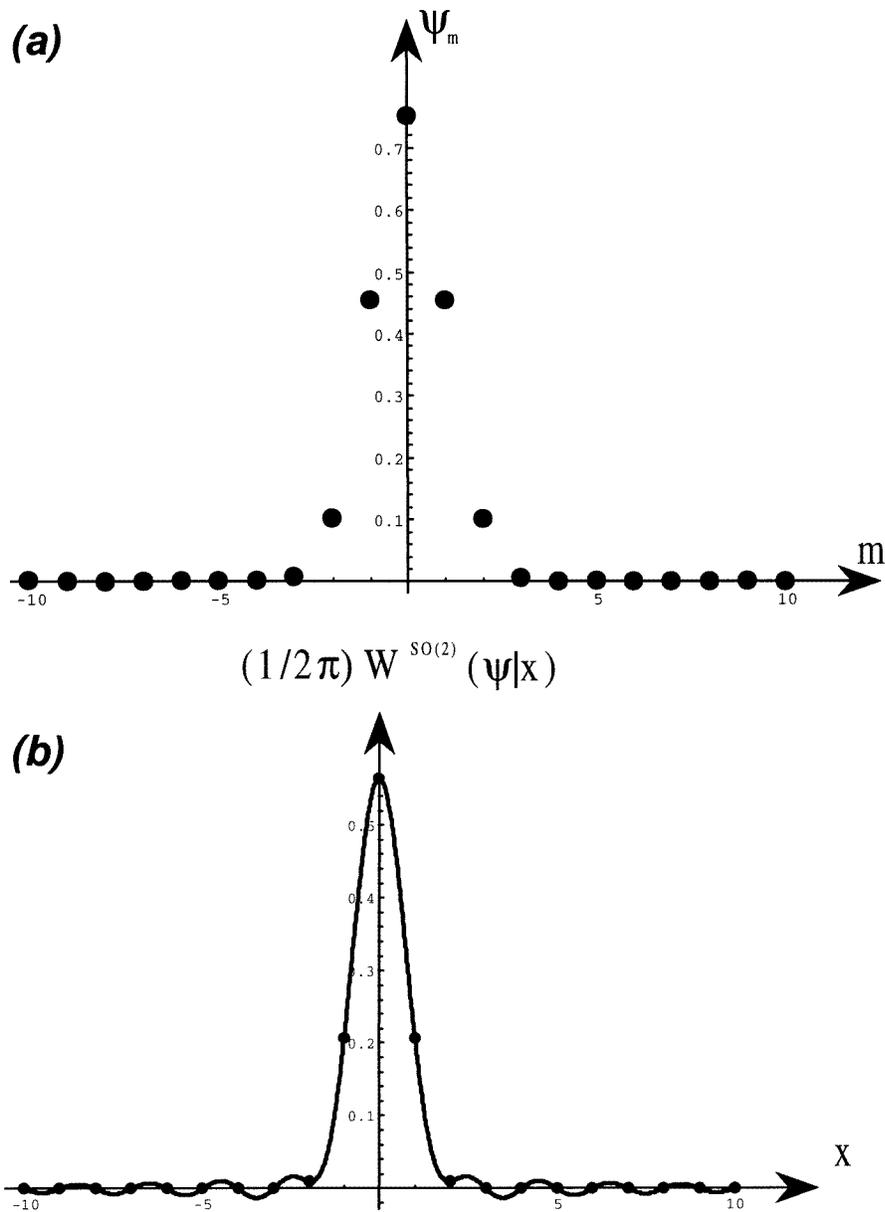
obtaining

$$W^{\mathrm{SO}(2)}(\phi, \psi|x) = \int_{\mathcal{S}_1} \mathrm{d}\gamma \, \mathrm{e}^{-\mathrm{i}\gamma x}(\phi^{0*} * \psi^\circ)[\gamma] \tag{2.8}$$

where $*$ is the convolution over $\mathcal{S}_1$. (Again we note that the exponential function in (2.8) is not periodic, i.e. single-valued, on $\mathcal{S}_1$.)

Thus in $\mathcal{L}^2(\mathcal{S}_1)$, the generator Q has the (non-diagonal) form $-\mathrm{i}\mathrm{d}/\mathrm{d}\theta$, and generates proper *rotations*: $g[\gamma]\psi^\circ(\theta) = \psi^\circ(\theta + \gamma)$. By covariance (1.6), we see that

$$W^{\mathrm{SO}(2)}(g(\alpha)\phi, g(\alpha)\psi|x) = W^\circ(\phi, \psi|x). \tag{2.9}$$

The Wigner function does not, therefore, distinguish between neither wavefunctions on the circle that are rotated by α, nor functions on the integers $\mathbb{Z}$ multiplied by phases $\mathrm{e}^{\mathrm{i}m\alpha}$. We

(a)

$$(1/2\pi)\, W^{SO(2)}(\psi|x)$$

(b)

Figure 1. (*a*) A function ψ_m on the integers $m \in \mathbb{Z}$. (*b*) Its Wigner function $W^{SO(2)}(\psi|x)$ of the continuous variable x (marked at the integer points, where it is $|\psi_m|^2$). Note that there are small intervals where the Wigner function is negative.

conclude that any dynamical process generated by a self-adjoint Hamiltonian $h(Q)$ (such as $\pm Q$ itself for wave propagation in a one-dimensional medium) leaves the SO(2) Wigner function invariant.

On the other hand, there are dynamical processes, such as heat diffusion in a conducting ring, generated by the non-unitary operator $\exp(-\tau Q^2)$, which do change the shape of the

Wigner function. In $\ell^2(\mathbb{Z})$ this multiplies each ψ_m, $m \in \mathbb{Z}$ by a factor

$$\Theta_m(\tau) = \exp(-m^2\tau) \tag{2.10a}$$

to produce $\psi_m(\tau) = \psi_m e^{-m^2\tau}$. The corresponding functions on the circle convolve with the diffusion kernel ([6, pp 170, 198 *et seq.*], see figure 4.13)

$$\Theta(\theta; \tau) = \frac{1}{\sqrt{2\pi}} \sum_{m\in\mathbb{Z}} e^{-m^2\tau+im\theta} = \frac{1}{2\pi} \vartheta_3\left(\frac{1}{2}\theta, e^{-\tau}\right) \tag{2.10b}$$

where $\vartheta_3(\cdot, \cdot)$ is the third Jacobi theta function [7]. These expression will be used below for Gaussians beams in optical wavefields.

3. The Euclidean algebra and group

In this section we review some useful properties of the two-dimensional Euclidean algebra e_2 and group E_2, in order to fix notation and gather some formulae that will be necessary to find the Wigner function on the Euclidean group.

3.1. Realizations of the Euclidean algebra

On the Hilbert space of square-summable sequences $\ell^2(\mathbb{Z})$, the Euclidean algebra (1.14) has a representation by self-adjoint difference operators with diagonal Q, given by

$$Q^{\mathbb{Z}}\psi_m = m\psi_m \qquad P^{\mathbb{Z}}\psi_m = -i\tfrac{1}{2}k[\psi_{m+1} - \psi_{m-1}] \qquad H^{\mathbb{Z}}\psi_m = \tfrac{1}{2}k[\psi_{m+1} + \psi_{m-1}] \tag{3.1}$$

for any $k > 0$. Through the synthesis of Fourier series (cf section 2.3), we have the following self-adjoint (multiplier) realization on differentiable functions $\psi(\theta)$ dense in $\mathcal{L}^2(\mathcal{S}_1)$,

$$Q^{\mathcal{S}} = -i\frac{d}{d\theta} \qquad P^{\mathcal{S}} = k\sin\theta \qquad H^{\mathcal{S}} = k\cos\theta. \tag{3.2}$$

These are two realizations of the unitary irreducible representation k of the Euclidean group, characterized by the value k^2 of the quadratic invariant operator $P^2 + H^2$, which plays the role of the Casimir operator for E_2. The Plancherel integral and measure over the harmonic conjugate unirrep space is $\int_0^\infty k\,dk\,\ldots$.

The prototypical realization of the Euclidean algebra, acting on differentiable functions $f(\boldsymbol{x})$ over the two-dimensional plane $\boldsymbol{x} = (x_1, x_2)$, dense in $\mathcal{L}^2(\mathbb{R}^2)$ and containing all unirreps, is given by the well known self-adjoint operators

$$Q^{\mathbb{R}^2} = -i\left(x_2\frac{\partial}{\partial x_1} - x_1\frac{\partial}{\partial x_2}\right) \qquad P^{\mathbb{R}^2} = -i\frac{\partial}{\partial x_1} \qquad H^{\mathbb{R}^2} = -i\frac{\partial}{\partial x_2}. \tag{3.3}$$

The connection between the realizations (3.1)–(3.3) will be given below.

3.2. Group manifold in coset coordinates

Rigid motions of the plane can be parametrized by one rotation $\rho \in \mathcal{S}_1$ and two orthogonal translations $\boldsymbol{s} = (s_1, s_2) \in \mathbb{R}^2$, that we conveniently treat as a two-dimensional row vector. We shall use the following presentation:

$$g\{\rho; \boldsymbol{s}\} = g\{\rho; 0\}\,g\{0; \boldsymbol{s}\} = \exp(i\rho Q)\exp(i[s_1 P + s_2 H]) \longrightarrow \mathbf{D}^{\mathrm{ad}}(g\{\rho; \boldsymbol{s}\})$$

$$= \begin{pmatrix} 1 & s_1 & s_2 \\ 0 & \cos\rho & -\sin\rho \\ 0 & \sin\rho & \cos\rho \end{pmatrix}. \tag{3.4}$$

We call these *coset* coordinates and indicate function arguments of them by *braces*. The product of two Euclidean group elements in coset coordinates is simplest:

$$g\{\rho; s\}\, g\{\rho'; s'\} = g\{\rho + \rho'; s\mathbf{R}(\rho') + s'\} \qquad \mathbf{R}(\rho) = \begin{pmatrix} \cos\rho & -\sin\rho \\ \sin\rho & \cos\rho \end{pmatrix}. \qquad (3.5)$$

The unit element is $e = g\{0; \mathbf{0}\}$, associativity holds, and the inverse of $g\{\rho; s\}$ is $g^{-1}\{\rho; s\} = g\{-\rho; -s\mathbf{R}(-\rho)\}$.

The Euclidean group is the semidirect product of two subgroups: the SO(2) subgroup of rotations, $g\{\rho; \mathbf{0}\}$, $\rho \in \mathcal{S}_1$, and the T_2 translation group $g\{0; s\}$, $s = (s_1, s_2) \in \mathbb{R}^2$. Figure 2 shows the realization of the Euclidean group of motions of the plane in the coset decomposition (3.4), (3.5): given a *standard frame*, each group element maps it to a distinct frame with origin at s and rotated by the angle ρ. We can picture the three-dimensional manifold of $g\{\rho; s\}$ as the set of all such rotated frames in 2-space. A *right coset* by the first of these groups is the (equivalence) set $\{g\{\rho; s\}\}_{\rho \in \mathcal{S}_1}$ of frames with the same origin s. The *space of cosets* is thus $s \in \mathbb{R}^2$, i.e. the set of origin points in the plane. In these coordinates, the invariant *Haar* integral is
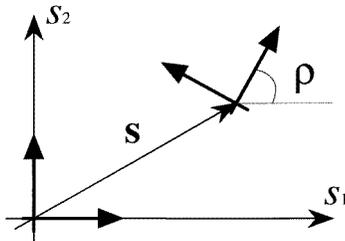
$$\int_{E_2} \mathrm{d}g f(g) = \int_{\mathcal{S}_1} \mathrm{d}\rho \int_{\mathbb{R}^2} \mathrm{d}s_1\, \mathrm{d}s_2\, f\{\rho; s_1, s_2\}. \qquad (3.6)$$

3.3. Group manifold in polar coordinates

The group E_2 also has the following presentation in *polar* coordinates:

$$g[\rho\boldsymbol{\xi}] = \exp\mathrm{i}(\rho Q + \xi_1 P + \xi_2 H) \longrightarrow$$

$$\mathbf{D}^{\mathrm{ad}}[\rho; \boldsymbol{\xi}] = \begin{pmatrix} 1 & \xi_1 \operatorname{sinc}\rho + \xi_2(\frac{1-\cos\rho}{\rho}) & -\xi_1(\frac{1-\cos\rho}{\rho}) + \xi_2 \operatorname{sinc}\rho \\ 0 & \cos\rho & -\sin\rho \\ 0 & \sin\rho & \cos\rho \end{pmatrix} \qquad (3.7)$$

where we indicate polar coordinates by the brackets. From (3.4) and (3.7), we find that $\xi_1 = \frac{1}{2}\rho(s_1 \cot\frac{1}{2}\rho - s_2) = s\sin(\sigma - \frac{1}{2}\rho)/\operatorname{sinc}\frac{1}{2}\rho$ and $\xi_2 = \frac{1}{2}\rho(s_1 + s_2 \cot\frac{1}{2}\rho) = s\cos(\sigma - \frac{1}{2}\rho)/\operatorname{sinc}\frac{1}{2}\rho$, where we define the polar coordinates of the vector $\mathbf{s}$ by $(s_1, s_2) = (s\sin\sigma, s\cos\sigma) = s[s, \sigma]$.

Figure 2. The group element $g\{\rho; s\} \in E_2$ in the coset parameters $\rho \in \mathcal{S}_1$, $s \in \mathbb{R}^2$, is pictured as the standard frame at the origin (boldface), translated by s and rotated by ρ.

From (3.6) and (3.7) follows the invariant Haar measure and integral in polar coordinates,

$$\int_{E_2} \mathrm{d}g f(g) = \int_{\mathcal{S}_1} (\operatorname{sinc}\tfrac{1}{2}\rho)^2 \,\mathrm{d}\rho \int_{\mathbb{R}^2} \mathrm{d}\xi_1\, \mathrm{d}\xi_2\, f[\rho\xi_1, \xi_2]. \qquad (3.8)$$

This integral is needed to build the Wigner operator (1.2).

3.4. Wigner operator on E_2

Let us call $(q, p, h) \in \mathbb{R}^3$ the real numbers that we make correspond to the generators Q, P and H of the Euclidean algebra. Then, the Wigner operator (1.2) is written in polar coordinates as follows

$$\mathcal{W}^{E_2}(q, p, h) = \int_{\mathcal{S}_1} (\text{sinc}\, \tfrac{1}{2}\rho)^2 \, \mathrm{d}\rho \int_{\mathbb{R}^2} \mathrm{d}^2\boldsymbol{\xi} \exp[-\mathrm{i}(q\rho + p\xi_1 + h\xi_2)]g[\rho\boldsymbol{\xi}]. \tag{3.9}$$

In this paper we find it more convenient to use coset coordinates. The Wigner operator (3.9) is re-expressed by rewriting the exponent in coset coordinates. Using radii and angles, defined by $(p, h) = (r \sin\alpha, r \cos\alpha) = \boldsymbol{r}[r, \alpha]$, the Wigner operator is

$$\mathcal{W}^{E_2}(q, \boldsymbol{r}[r, \alpha]) = \int_{\mathcal{S}_1} \mathrm{d}\rho \int_0^{\infty} s \, \mathrm{d}s \int_{\mathcal{S}_1} \mathrm{d}\sigma$$
$$\times \exp\left[-\mathrm{i}\rho\left(q + rs \frac{\cos(\alpha - \sigma + \tfrac{1}{2}\rho)}{2\sin\tfrac{1}{2}\rho}\right)\right] g\left\{\rho; \boldsymbol{s}[s, \sigma]\right\}. \tag{3.10}$$

This operator can be applied to functions over the group, or over any homogeneous space under the group, and integrated with a second such function, to produce their mutual Wigner *function* (1.3).

4. Euclidean discrete optics

Euclidean optics contain at least two models: the realization (3.1) of the Euclidean algebra by difference operators on the Hilbert space $\ell^2(\mathbb{Z})$ leads naturally to the *discrete* model of this section; the realizations (3.2) and (3.3) on $\mathcal{L}^2(\mathcal{S}_1)$ correspond to the 'continuous' wave optics model, including Helmholtz optics for a definite unirrep, that will be examined in the next section.

4.1. The discrete model

The operator Q is associated to the position variable of Euclidean systems that satisfy Newton's equation $\ddot{q} = 0$ in (1.10). The corresponding Lie–Newton equation involves the double commutator of operators, acting on $\ell^2(\mathbb{Z})$ wavefunctions that are infinite column vectors $\boldsymbol{\psi} = \{\psi_m\}_{m \in \mathbb{Z}}$ (where we omit the $\mathbb{Z}$ superscript). This equation in the discrete optics model is

$$[H, [H, Q]]\boldsymbol{\psi} = (HHQ - 2HQH + QHH)\boldsymbol{\psi} = \ddot{\boldsymbol{\psi}} = 0 \tag{4.1a}$$

i.e. $\ddot{\psi}_m = \tfrac{1}{4}k^2[(m\psi_{m+2} + 2m\psi_m + m\psi_{m-2}) - ((m+1)\psi_{m+2} + 2m\psi_m$
$$+ (m-1)\psi_{m-2} + (m+2)\psi_{m+2} + 2m\psi_m + (m-2)\psi_{m-2})] \equiv 0. \tag{4.1b}$$

This is satisfied identically by the generators (3.1), namely

$$Q\psi_m = m\psi_m \qquad m \in \mathbb{Z} \tag{4.2a}$$
$$P\psi_m = -\mathrm{i}\tfrac{1}{2}k(E^{\uparrow} - E^{\downarrow})\psi_m \qquad H\psi_m = \tfrac{1}{2}k(E^{\uparrow} + E^{\downarrow})\psi_m \tag{4.2b}$$

where

$$E^{\uparrow\downarrow} = k^{-1}(H \pm \mathrm{i}P) \qquad E^{\uparrow\downarrow}\psi_m = \psi_{m\pm 1}. \tag{4.3}$$

Therefore the operators of the algebra are self-adjoint under the usual inner product $(\boldsymbol{\psi}, \boldsymbol{\phi})_{\ell^2} = \sum_{m \in \mathbb{Z}} \psi_m^* \phi_m$.

Notice very carefully that the discrete Lie–Newton equation (4.1) for any ψ_m involves only its *second*-neighbour points $\psi_{m\pm2}$, and not at all the first-neighbour ones $\psi_{m\pm1}$. We conclude that the subvectors $\{\psi_m\}_{m \text{ even}}$ and $\{\psi_m\}_{m \text{ odd}}$ are two independent solutions for discrete homogeneous optical media. The quadratic invariant operator in the realization (3.1) is a fixed multiple by $k \in \mathbb{R}^+$ of the unit operator in $\ell^2(\mathbb{Z})$,

$$K^2 = P^2 + H^2 = k^2 \mathbf{1}. \tag{4.4}$$

Its eigenvalues $k^2 \geqslant 0$ classify the unirreps of E_2. The Plancherel direct integral and measure is $\int_0^\infty k \, dk \cdots$. The $k = 0$ representation (limit of geometric optics) has zero measure by this decomposition.

The $\ell^2(\mathbb{Z})$-normalized eigenfunctions of the position operator Q in this model are the *localized* states $\psi^{(m_0)} = \{\psi_m^{(m_0)}\}_{m\in\mathbb{Z}}$, where $\psi_m^{(m_0)} = \delta_{m_0,m}$, corresponding to the integer eigenvalues $m_0 \in \mathbb{Z}$. In the discrete model, the physical position values are $q = m/k = m\bar{\lambda}$, where $\bar{\lambda} = \lambda/2\pi = 1/k$ is the *reduced wavelength* of the wavefield; we understand these as the 'sensor' points of the field amenable to observation.

4.2. Evolution of the discrete wavefield

Consider the evolution of wavefunctions under the operator $\exp(izH)\psi_m$ (where z has units of $1/k = \bar{\lambda}$ so the exponent be dimensionless). We identify z with the translation parameter along an 'optical axis' which is perpendicular to the axis of positions in a two-dimensional physical medium. We compute

$$(H^n\psi)_m = \frac{k^n}{2^n} \sum_{j=0}^n \binom{n}{j} (E^{\uparrow j} E^{\downarrow(n-j)}\psi)_m = \frac{k^n}{2^n} \sum_{j=0}^n \binom{n}{j} \psi_{m+2j-n} \tag{4.5}$$

to find the *propagator* of discrete Euclidean optical systems,

$$\psi_m(z) = (\exp(izH)\psi)_m = \sum_{n\in\mathbb{Z}} i^n J_n(kz)\psi_{m+n}. \tag{4.6}$$
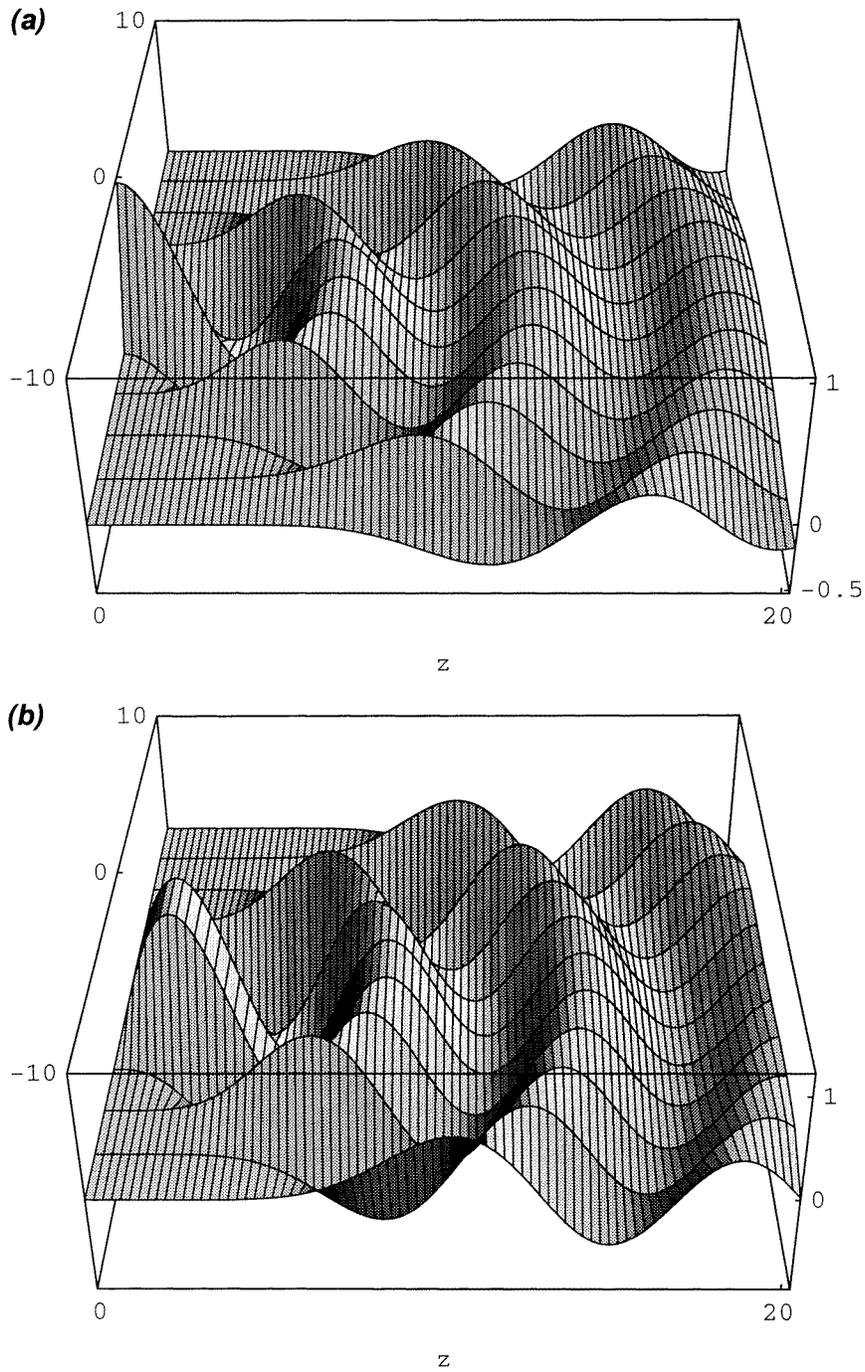
4.3. Wavefield values and normal derivatives

Recall that at even and odd points m, the ψ_m's satisfy independent second-order wave equations. Note that since $J_{-n}(kz) = (-1)^n J_n(kz) = J_n(-kz)$, the factor of ψ_{m+n} in (4.6) with n even, is even under z-reflection, and odd for n odd. This symmetry corresponds to the evolution of initial values and of initial normal derivatives in a wave medium, respectively $\{\psi_m\}_{m \text{ even}}$ and $\{\psi_m\}_{m \text{ odd}}$. Consider the initial *Gaussian* wavefunction in $\ell^2(\mathbb{Z})$ given by

$$\mathbf{\Gamma}_{m_0,\alpha}^\omega = \sum_m \Gamma_{m-m_0}^\omega e^{im\alpha}\psi^{(m)} \qquad \Gamma_m^\omega = \exp(-m^2/2\omega) \tag{4.7}$$

centred at $m_0 = 0$, of angle $\alpha = 0$, and of width ω. Here $\psi^{(m)}$ are the basis vectors, which in the realization (2.7) are $e^{im\theta}$. In figure 3(*a*) we interpolated graphically between integer, even m's, while figure 3(*b*) shows the waveforms obtained from interpolation between the companion odd values of m.

The interpretation of initial values and normal derivatives on alternating even and odd points in discrete system appears novel; it is further supported by the following consideration: the z-derivative of the exponential series reproduces the series, acted upon by iH. At $z = 0$, the normal derivative of ψ is

$$\psi_m' = \frac{\partial}{\partial z} \psi_m(z)|_{z=0} = i(H\psi)_m = i\tfrac{1}{2}k(\psi_{m+1} + \psi_{m-1}). \tag{4.8}$$

Figure 3. Discrete waveforms in the q–z plane obtained from the initial condition $\psi^{(0)}$ (a single 1 at $m = 0$) under z-evolution generated by the discrete optical Hamiltonian (4.6). (a) Interpolating linearly between even-m points; and (b) between odd-m points. The former are intepreted as field values and the latter as the z-normal derivatives.

The dichotomy of alternating points reminds us of the $2N$ classical position and momentum variables of finite mechanical vibrating lattices of N masses [6] on one hand, and of the determination of Helmholtz wavefields by two functions: values and normal derivatives, on a (continuous) line, on the other hand. This dichotomy is preserved under translations of the plane, since $g\{0; s\}$ commutes with $\exp(\mathrm{i}zH)$ (see (3.4)–(3.7)), but not under rotations of the plane $g\{\rho; \mathbf{0}\}$. These observations apply for other discrete systems governed by second-order differential-difference Newton equations.

4.4. Wigner matrix in discrete optics

In this E_2 model of discrete optics, the sensors read the field values ψ_m. To find the analytic form of the Wigner function we need the action of E_2 on the basis $\{\psi^{(m)}\}_{m\in\mathbb{Z}}$.

Under rotations of the plane generated by Q, vectors $\psi \in \ell^2(\mathbb{Z})$ transform as $g\{\rho; \mathbf{0}\}\,\psi_m = \mathrm{e}^{\mathrm{i}m\rho}\psi_m$. Under translations along the z-axis by H, the action was found in terms of the Bessel functions in equation (4.8). Translations by s along any line with angle σ (anticlockwise from the z-axis) are thereby produced through the similarity transformation $g\{-\sigma; \mathbf{0}\}\,g\{0; 0, s\}\,g\{\sigma; \mathbf{0}\} = g\{0; s\sin\sigma, s\cos\sigma\}$. In coset coordinates (3.4) we write

$$g\{\rho; s\sin\sigma, s\cos\sigma\}\,\psi_m = \sum_{n\in\mathbb{Z}} E^k_{m,n}\{\rho; s\sin\sigma, s\cos\sigma\}\,\psi_n \tag{4.9a}$$

where

$$E^k_{m,n}\{\rho; s\sin\sigma, s\cos\sigma\} = \mathrm{i}^{m-n}\mathrm{e}^{\mathrm{i}m\rho}J_{m-n}(ks)\mathrm{e}^{\mathrm{i}(n-m)\sigma} \tag{4.9b}$$

are the unirrep matrix elements. In [9], sections 4.1.2, 4.1.3 and 4.4.1, we denote them by E instead of D and use a different phase convention. Note that equation (4.6) is a particular case of equation (4.9) when $\sigma = 0 = \rho$.

The orthonormal basis of localized wavefunctions, $\{\psi^{(m)}\}_{m\in\mathbb{Z}}$, allows us to write vectors as $\phi = \sum_{m\in\mathbb{Z}}\phi_m\psi^{(m)}$. The Wigner function can then be written as

$$W(\phi, \chi|q, p, h) = \sum_{m,n\in\mathbb{Z}} \phi_m^* W_{m,n}(q, p, h)\chi_n \tag{4.10a}$$

where the *Wigner matrix* $W_{m,n}(q, p, h)$ is obtained by inner product of the Wigner operator between the basis states m and n,

$$W_{m,n}(q, p, h) = (\psi^{(m)}, \mathcal{W}(q, p, h)\psi^{(n)})_{\ell^2(\mathbb{Z})}. \tag{4.10b}$$

In (3.10), the abstract group element $g\{\rho; s[s, \sigma]\}$ is replaced by the unirrep matrix elements (4.9), $E^k_{m,n}\{\rho; s[s, \sigma]\}$; the rightmost integral is

$$\frac{1}{2\pi}\int_{\mathcal{S}_1}\mathrm{d}\sigma \exp\left(-\mathrm{i}rs\frac{\cos(\alpha - \sigma + \frac{1}{2}\rho)}{\mathrm{sinc}\,\frac{1}{2}\rho}\right)\mathrm{e}^{\mathrm{i}(n-m)\sigma} = \mathrm{i}^{m-n}\mathrm{e}^{\mathrm{i}(n-m)(\alpha+\rho/2)}J_{n-m}(rs/\mathrm{sinc}\,\tfrac{1}{2}\rho). \tag{4.11a}$$

Next, the radial integral is performed over s; its integrand has two Bessel functions: one $J_{m-n}(ks)$ and another from (4.11a). We recall the formula

$$\int_0^\infty s\,\mathrm{d}s\,J_n(k_1s)J_n(k_2s) = k_1^{-1}\delta(k_1 - k_2) \tag{4.11b}$$

to reduce the Wigner matrix elements to

$$W_{m,n}(q, \mathbf{r}[r, \alpha]) = \mathrm{e}^{\mathrm{i}(n-m)\alpha}\frac{2\pi}{k}\int_{\mathcal{S}_1}\mathrm{d}\rho\,\delta\left(\frac{r}{\mathrm{sinc}\,\frac{1}{2}\rho} - k\right)\exp(\mathrm{i}\rho[\tfrac{1}{2}(n+m) - q]). \tag{4.12}$$

(Again the integrand is not 2π-periodic in ρ.) The Dirac δ picks out the symmetric roots

$$\operatorname{sinc} \tfrac{1}{2}(\pm\rho_0) = r/k. \tag{4.13}$$

Since the maximum value of the sinc function is at $\operatorname{sinc} 0 = 1$, when $r > k$ there is no root and the Wigner function is zero. For $0 > r > k$ the sinc function in (4.13) provides one or more pairs of roots $\pm\rho_0$, since $\operatorname{sinc} \tfrac{1}{2}\tau$, $\tau > 0$ has maxima at $\tau_n^{\max} = 0, 5\pi, 7\pi, \ldots, (2n+1)\pi, \ldots$ ($n = 1, 2, 3, \ldots$) with values $1, 2/5\pi, 2/7\pi, \ldots, 2/(2n+1)\pi$. If $r/k < 2/(2n+1)\pi$, (4.13) will provide a couple of roots ρ_0 due to the nth maximum, and also a couple around all other $\tau_m^{\max}$, $1 < m < n$, plus one root in the central positive lobe of the sinc function, i.e. the interval $0 < \tau < 2\pi$.

Since the angle ρ corresponds to the rotation angle of the standard frame in figure 2, we see that its extension beyond the basic interval $-\pi < \rho \leqslant \pi$ of the circle $\mathcal{S}_1$ presents features similar to the SO(2) case studied in section 2.2. The interpretation we follow here is that we can choose the *double cover* group of E_2, denoted $E_2^{(2)}$ and characterized by $-2\pi < \rho < 2\pi$, to accomodate for the main lobe of the sinc function with a single pair of roots of (4.13) for $0 < r < k$ at $\pm\rho_0$ in that interval. Finally, when $r/k = 1$, the two symmetric roots $\pm\rho_0$ coalesce to a double root at 0. The Wigner matrix elements on $E_2^{(2)}$ are thus found in closed form:

$$W_{m,n}(q, \boldsymbol{r}[r, \alpha]) = \begin{cases} e^{\mathrm{i}(n-m)\alpha} \dfrac{4\pi r\rho_0}{k^2} \dfrac{\sin\tfrac{1}{2}\rho_0 \cos\rho_0(\tfrac{1}{2}(n+m) - q)}{r - k\cos\tfrac{1}{2}\rho_0} & r < k \\ 0 & r > k. \end{cases} \tag{4.14a}$$
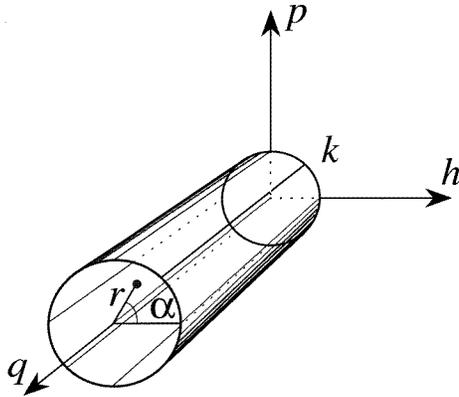
When r approaches k from below, then $\rho_0 \sim \sqrt{24(1 - r/k)}$, and the Wigner function has the singularity

$$\lim_{r \to k^-} W_{m,n}(q, \boldsymbol{r}[r, \alpha]) = \frac{24\pi}{\sqrt{6}k^{3/2}} \frac{e^{\mathrm{i}(n-m)\alpha}}{\sqrt{k - r}} \tag{4.14b}$$

which is integrable in r and in k over $\int_0^k r \, \mathrm{d}r$ and $\int_0^\infty k \, \mathrm{d}k$. Indeed, below we shall integrate (4.12) over r *first*, so the Dirac δ will set $r = k \operatorname{sinc} \tfrac{1}{2}\rho$ with ρ in the same interval.

4.5. Marginal distribution of the Wigner function on the cylinder

The Wigner function (4.10)–(4.14) of this discrete wavefunction should be plotted in three-dimensional space; as shown in figure 4, it is zero outside the cylinder of axis $(q, 0, 0)$ and radius $k = \sqrt{p^2 + h^2}$, which is determined by the unirrep label $k = \lambdabar^{-1} \in \mathbb{R}^+$, the wavenumber of the field. The Wigner function oscillates strongly with the radius r, except for a stationary point $q = m_0/k$ at the centre of the wavefunction, and has an inverse-square-root singularity at the surface of the cylinder. For the model at hand, this indicates that three dimensions is more than needed—and convenient—for plotting the Wigner function. In D-dimensional quantum mechanics ($D \geqslant 2$), two common resorts are to slice or to project the Wigner functions onto lower-dimensional spaces; the latter are the *marginal distributions*. In [3, 4] we used the former for SU(2), having found that the largest values of the Wigner function are in a spherical shell between radii ℓ and $\ell + 1$, with an absolute maximum at $\sqrt{\ell(\ell + 1)}$; so we chose there to present the plots of the Wigner function on that spherical section. Now, the $E_2^{(2)}$ group is the contraction $c \to 0$ of SU(2) with $\ell = k/c \to \infty$ and angles $\theta = s/\ell$ becoming the translation parameter s. The result of this contraction is that the SU(2) Wigner function will concentrate on the boundary of the limit cylinder, producing the $(r - k)^{-1/2}$ sigularity. (Further study of this and the Heisenberg–Weyl limits will be considered elsewhere.)

Figure 4. The Wigner function $W(\psi|q, p, h)$ on three-dimensional space (q, p, h) is different from zero inside a cylinder whose axis is $(q, 0, 0)$ and whose squared radius is $p^2 + h^2 = k^2$, determined by the unirrep label $k = \lambda^{-1} \in \mathbb{R}^+$. On the surface of the cylinder there is an inverse-square-root singularity.

To visualize the information contained in the Wigner function on (q, p, h), our strategy here will be to project it onto a *marginal distribution* on lower-dimensional subspace. We have found particularly attractive the radial projection of the plane $(p, h) = \boldsymbol{r}[r, \alpha]$, i.e. integrating over r and using $\mathrm{d}r = \mathrm{d}\rho(k \cos \frac{1}{2}\rho_0 - r)/\rho_0$

$$M(\phi, \chi|q, \alpha) = \int_0^\infty r \, \mathrm{d}r \, W(\phi, \chi|q, \boldsymbol{r}[r, \alpha]) = 4\pi \sum_{m,n \in \mathbb{Z}} \phi_m^* \mathrm{e}^{\mathrm{i}(n-m)\alpha} Z(\tfrac{1}{2}[n+m] - q)\chi_n$$
$$(4.15a)$$

where (cf equation (2.6))

$$Z(\mu) = \int_0^{2\pi} \mathrm{d}\rho(\mathrm{sinc}\,\tfrac{1}{2}\rho)^2 \cos \mu\rho. \qquad (4.15b)$$

In figure 5 we show the marginal distribution (4.15) of the 'Gaussian' vector (4.7) as a function of $q \in \mathbb{R}$ and $\alpha \in \mathcal{S}_1$. The function $Z(\mu)$ in (4.15b) is shown in figure 6; it has a role very similar to the sinc interpolant of the Wigner function on SO(2). Note that it is even and $\int_{\mathbb{R}} \mathrm{d}\mu Z(\mu) = \pi$. The $Z(\mu)$ function is, however, broader than the sinc, less negative, and is very small—but not strictly zero—at the non-zero integers. The first seven zeros of the function $Z(\mu)$, for $\mu > 0$ are:
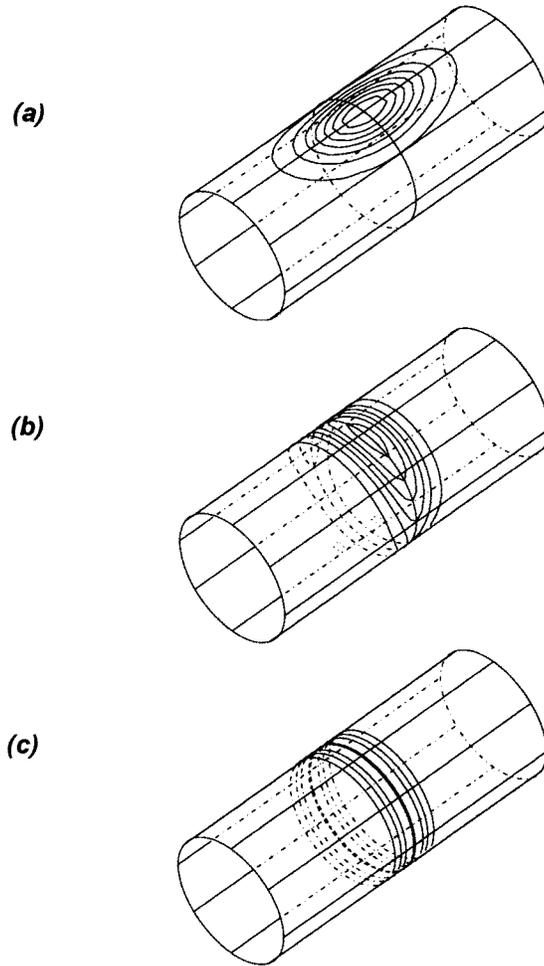
$$1.1719, 1.6066, 2.0781, 2.5619, 3.0513, 3.5438, 4.0384.$$

They can be compared with the zeros of the function $\mathrm{sinc}\,2\pi\mu$, which occur for integer and half-integer values of μ.

Because of its sesquilinearity, the marginal distribution (4.15) of Schrödinger cat states $\phi + \chi$ contains three terms:

$$M(\phi + \chi|q, \alpha) = M(\phi|q, \alpha) + M(\chi|q, \alpha) + 2\mathrm{Re}M(\phi, \chi|q, \alpha). \qquad (4.16)$$

The first two terms are the Wigner function of the constituent states of the cat, while the third, termed the *smile* of the cat state, bears their Moiré pattern, a highly oscillating region between the two due to their mutual inteference. In figure 7 we show the Wigner functions of cat states composed of two Gaussian wavefields. In figure 7(a) the cat state is $\mathrm{e}^{-(m-m_0)^2/2\omega} + \mathrm{e}^{-(m+m_0)^2/2\omega}$, i.e. two parallel Gaussians centred at $\pm m_0$; the smile exhibits
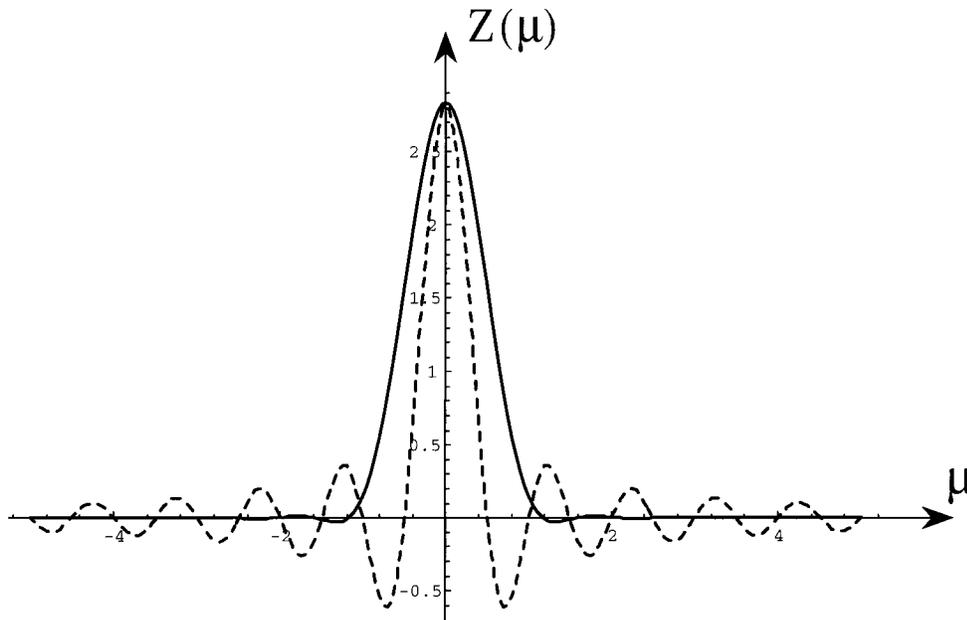
(a)

(b)

(c)

Figure 5. Marginal distribution on the cylinder of the Wigner function of Gaussian vectors (4.7), centred at $m_0 = 0$ and direction $\alpha = 0$, of width ω. (*a*): $\omega = 0.1$ (a very broad Gaussian—almost a plane wave of definite direction $\alpha = 0$). (*b*) $\omega = 1$ (the Gaussian wavefield composed of the initial values in figure 3(*a*) and normal derivatives in figure 3(*b*)). (*c*) $\omega = 10$ (a very narrow-waisted Gaussian—almost a localized state at $m_0 = 0$).

groves ('teeth') along the axis of the cylinder, with the highest oscillations in α around the midpoint $q = 0$. In figure 7(*b*) the cat state consists of two Gaussians with the same centre and waist, but differing by their angles: $(e^{im\alpha_1} + e^{-im\alpha_2})e^{-m^2/2\omega}$; the smile now has its teeth across the cylinder axis, with highest oscillations in q, at the angle bisecting the two Gaussian beams.

Integration of the cylinder marginal distribution (4.15) over angles $\alpha \in \mathcal{S}_1$ produces a marginal distribution in position q alone. Further integrating the marginal distribution (4.15*a*) over $\int_0^k r \, dr \ldots$, we obtain

$$M(\phi, \chi|q) = \int_{\mathbb{R}^2} dp \, dh \, W(\phi, \chi|q, p, h) = 8\pi^2 \sum_{m \in \mathbb{Z}} \phi_m^* Z(m - q)\chi_m. \quad (4.17)$$

This may be compared with the SO(2) Wigner function in equation (2.5): they are different,

Figure 6. The function $Z(\mu)$ in (4.15*b*) (full curve) compared with the function sinc $2\pi\mu$ (broken curve), normalized to the same value at the maximum $\mu = 0$.

indicating that the latter is not simply a restriction of the former. Finally, integrating (4.17) over $\int_{-\infty}^{\infty} dq \ldots$, gives

$$M(\phi, \chi) = \int_{\mathbb{R}^3} dq \, dp \, dh \, W(\phi, \chi | q, p, h) = 8\pi^3(\phi, \chi)_{\ell^2(\mathbb{Z})}. \tag{4.18}$$

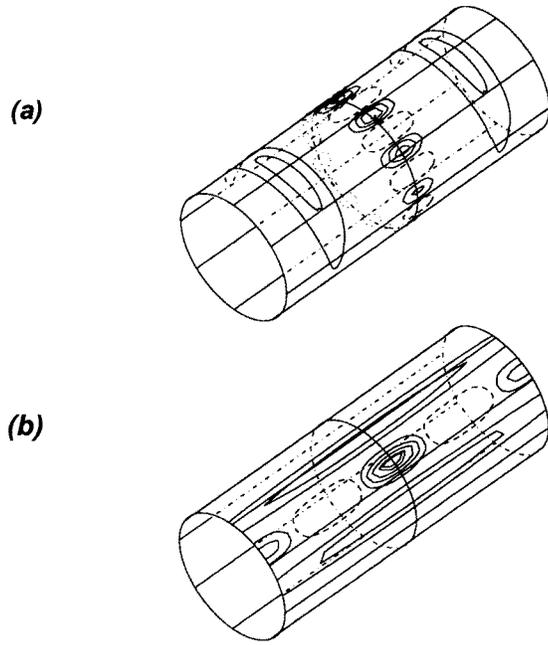### 4.6. Euclidean covariance of the Wigner function

When discrete wavefields, such as those of figures 3, are subject to Euclidean transformations, their Wigner function will transform covariantly according to equation (1.6). Meta-phase space (q, p, h) will follow the adjoint representation (3.4)–(3.7) of E_2.

Rotations generated by Q will multiply the components of the state ψ_m by phases $e^{im\beta}$; they will rotate its Wigner function (4.14) by $\alpha \to \alpha + \beta$ around the q-axis, and similarly for the marginal distribution (4.15). On the other hand, movement of the q-line of sensors along the z-axis generated by H and given in (4.6), corresponds to

$$W(\phi(z), \chi(z) | q, p, h) = W(\phi(0), \chi(0) | q + zh, p, h) \tag{4.19}$$

i.e. a linear slant in the q–h plane. Under P-evolution, the slant is in the q–p plane. These transformations map 1:1 the surface of each cylinder ($p^2 + h^2 = $ constant) onto itself.

The marginal distribution $M(\psi | q, \alpha)$ in (4.15), is geometrically covariant under rotations, but translations along z will smear the function in q, maximally in the $\alpha = 0$ direction. In figures 5 and 7, it will broaden the Gaussian peaks of the Wigner marginal distribution; their waist will be now off the $z = 0$ line.

Figure 7. Marginal distribution on the cylinder of the Wigner of Schrödinger cat states composed of two Gaussian vectors (4.7). (*a*) Two parallel narrow Gaussian beams separated in position. (*b*) Two overlapping wide Gaussian beams at different angles.

5. Wigner function for Helmholtz and polychromatic wavefields

In this section we shall use the realization of the Euclidean group (3.2) on the circle in momentum space and (3.3) in the plane. The first corresponds to the Helmholtz model of 2π monochromatic optics of wavenumber k, and the latter to the continuum of wavenumbers $k \in \mathbb{R}^+$ for colour wave optics. Although both of these closely related models have been subject to group-theoretical analysis as wave theories over N-dimensional Euclidean groups [8, 10], the Wigner function is introduced here for the first time.

5.1. The Helmholtz model of Euclidean optics

The E_2 quadratic invariant operator (4.4) for functions in the unirrep $k \in \mathbb{R}^+$, is

$$\left(\frac{\partial^2}{\partial x_1^2} + \frac{\partial^2}{\partial x_2^2} \right) \Psi^{(k)}(x_1, x_2) = -k^2 \Psi^{(k)}(x_1, x_2). \tag{5.1}$$

As is well known, square-integrable solutions of the Helmholtz equation (5.1) and their $\mathcal{L}^2(\mathbb{R}^2)$ limit points, have a two-dimensional Fourier transform with support on the circle of radius k, namely

$$\widetilde{\Psi}^{(k)}(r \sin \theta, r \cos \theta) = \mathcal{F}_{x \to r} \Psi^{(k)} = k^{-1} \delta(k - r) \psi(k, \theta). \tag{5.2}$$

Thus, the Helmholtz wavefields are described by complex functions on the circle, $\psi(k, \theta) \in \mathcal{L}^2(\mathcal{S}_1)$, for fixed k. Given a function $\psi(k, \theta)$ on the circle, its *wave synthesis* is

$$\Psi^{(k)}(x_1, x_2) = \int_{\mathcal{S}_1} d\theta \, \psi(k, \theta) \exp(ik[x_1 \sin \theta + x_2 \cos \theta]). \tag{5.3}$$

Such solutions to (5.1) are said to be of *oscillatory* type (exponential solutions cannot be represented in this way). The inverse transform to (5.3), its *wave analysis*, can be given in terms of values and normal derivatives of the field at a line screen $x_2 = 0$ [8, 10], by

$$\psi(k, \theta) = \frac{\tau}{2}\sqrt{\frac{k}{2\pi}} \int_{\mathbb{R}} dx_1 \left(\Psi^{(k)}(x_1, 0) \cos\theta + \frac{1}{ik} \frac{\partial \Psi^{(k)}(x_1, x_2)}{\partial x_2} |_{x_2=0} \right) \exp(-ikx_1 \sin\theta).$$

$$(5.4)$$

The action of an element of the Euclidean group on a Helmholtz wavefield $\Psi(x_1, x_2)$ consists of rigid translations and rotations of the optical x_1, x_2-plane. Correspondingly, on the representative functions on the circle $\psi(\theta)$, the realization (3.2) holds and its action consists of geometric and ray (phase) transformations,

$$g\{\rho; s\} \psi(k, \theta) = \exp(ik[s_1 \sin(\theta + \rho) + s_2 \cos(\theta + \rho)])\psi(k, \theta + \rho). \qquad (5.5)$$

As long as we have a definite value of k we are in the Helmholtz model, and will omit this unirrep label from the notation. It will be recovered in section 5.5.

5.2. Wigner operator and function on Helmholtz fields

The action of the Wigner operator (3.9) on functions on the circle (5.4) can be written as follows

$$\mathcal{W}(q, p, h)\psi(k, \theta) = \int_{\mathcal{S}_1} d\rho \int_{\mathbb{R}^2} d^2s e^{-i\rho q} \times \exp(is_1[k\sin(\theta + \rho) - \tfrac{1}{2}\rho(p \cot \tfrac{1}{2}\rho + h)])$$

$$\times \exp(is_2[k\cos(\theta + \rho) - \tfrac{1}{2}\rho(h \cot \tfrac{1}{2}\rho - p)])\psi(k, \theta + \rho)$$

$$= \frac{4\pi^2}{r} \int_{\mathcal{S}_1} d\rho \operatorname{sinc}^2 \tfrac{1}{2}\rho e^{-i\rho q} \delta(r - k \operatorname{sinc} \tfrac{1}{2}\rho)\delta(\theta - \alpha + \tfrac{1}{2}\rho)\psi(k, \theta + \rho). \quad (5.6)$$

In the last expression we use again the parametrization $(p, h) = (r \sin\alpha, r \cos\alpha) = r[r, \alpha]$ and we encounter again the two roots $\pm\rho_0 = 2\operatorname{arcsinc}(r/k)$ of (4.13), and employ the same arguments to use the main part of the sinc function.

Now the Wigner function can be built from (1.3a), (5.6), and the $\mathcal{L}^2(\mathcal{S}_1)$ inner product. The δ's eliminate all integrals and the Wigner function reduces to

$$W(\phi, \chi | q, r[r, \alpha]) = V_k(r)[e^{-i\rho_0 q}\phi(k, \alpha - \tfrac{1}{2}\rho_0)^*\chi(k, \alpha + \tfrac{1}{2}\rho_0)$$

$$+ e^{+i\rho_0 q}\phi(k, \alpha + \tfrac{1}{2}\rho_0)^*\chi(k, \alpha - \tfrac{1}{2}\rho_0)] \qquad (5.7a)$$

$$V_k(r) \begin{cases} \dfrac{8\pi^2}{k^2} \dfrac{\sin\tfrac{1}{2}\rho_0}{\operatorname{sinc}\tfrac{1}{2}\rho_0 - \cos\tfrac{1}{2}\rho_0} = \dfrac{4\pi^2}{k^2} \dfrac{\rho_0 r}{r - k\cos\tfrac{1}{2}\rho_0} & r < k \\ 0 & r > k \end{cases} \qquad (5.7b)$$

and when r approaches k from below,

$$\lim_{r \to k^-} V_k(r) = \frac{1}{\sqrt{k-r}} \frac{24\pi^2}{\sqrt{6}k^{3/2}}. \qquad (5.7c)$$

We observe that this Wigner function has the same general form as the common QM Wigner function—but with no integral.

The Helmholtz and discrete optics models are related by expansion (2.7) of the functions on the circle in Fourier series. The basis of localized wavefunctions of the discrete model $\psi^{(m_0)}$ (eigenfunctions of Q with eigenvalues $m_0 \in \mathbb{Z}$) are represented by a Kronecker δ_{m,m_0} in the discrete model; on the circle they are periodic functions $(2\pi)^{-1/2}e^{im_0\theta}$, corresponding to multipolar solutions in the Helmholtz optical plane (involving Bessel functions of index

m_0 in kr [6]). Plane waves in the Helmholtz model, of direction θ_0 (eigenfunctions of P and H with eigenvalues $k \sin \theta$ and $k \cos \theta$ respectively), are $\delta(\theta - \theta_0)$ on the circle; in the discrete model they are vectors with components $e^{im\theta_0}$. Indeed, through Fourier series, from (5.7) we find the Wigner function for the discrete optics model (4.10)–(4.14).

5.3. Marginal distribution on the cylinder

The projection (marginal distribution) of the Wigner function on the cylinder in the Helmholtz model is amenable to an analysis, parallel to that of the discrete optics model (in particular, the analysis we made following equation (4.13)). It is of a simpler form because it uses complex functions on the circle.

We integrate over the radius r in the (p, h)-plane to obtain the Wigner marginal distribution on the cylinder (q, α). It is

$$M(\phi, \chi | q, \alpha) = 4\pi^2 \int_{-2\pi}^{2\pi} d\rho \, (\text{sinc} \tfrac{1}{2}\rho)^2 \phi(k, \alpha - \tfrac{1}{2}\rho)^* e^{-i\rho q} \chi(k, \alpha + \tfrac{1}{2}\rho) \tag{5.8}$$

and can be compared with (4.15). The form of the arguments is familiar from QM (cf (1.8)). Observe the extra factor $(\text{sinc} \tfrac{1}{2}\rho)^2$, which is 1 at the centre of the interval and decreases to zero at the edges.

Rotation and translation of Helmholtz wavefields are geometric and phase transformations of the functions on the circle (5.5). Under Euclidean transformations, the Wigner function obeys covariance, as in section 4.5: the cylinder will rotate and slant. However, the *dynamics* of the discrete optics and Helmholtz models are different: in the former, the evolution Hamiltonian is the z-translation generator H; in the latter, *time* evolution of a Helmholtz field multiplies the wavefunctions by the phase $\exp(ickt)$, where c is the speed of the wave in the medium. The Helmholtz Wigner function (5.7) and marginal distribution (5.8) are insensitive to such phases, so they will be constant in time.

In particular, corresponding to the Gaussian vectors (4.7), we have the Jacobi theta functions over the circle [7],

$$\Gamma^\omega(\theta) = \frac{1}{2\pi} \vartheta_3 \left(\frac{1}{2}\theta, e^{-1/2\omega} \right) = \frac{1}{\sqrt{2\pi}} \sum_{m \in \mathbb{Z}} \exp(-m^2/2\omega + im\theta). \tag{5.9}$$

By (5.2) and (5.3), the Helmholtz Gaussian wavefields are, in polar coordinates,

$$\Gamma_\omega^{(k)}(x \sin \xi, x \cos \xi) = \frac{1}{\sqrt{2\pi}} \sum_{m=0}^{\infty} e^{-m^2/2\omega} J_m(kx) \cos(m(\xi + \tfrac{1}{2}\pi)). \tag{5.10}$$

The Wigner functions shown in figures 5 and 7 correspond to such waveforms.

5.4. Polychromatic wave optics

Solutions to the two-dimensional wave equation include all wavenumbers $k \in \mathbb{R}^+$ and the wavefunctions are generalized sums of solutions to Helmholtz equations with this range of k with measure $k \, dk$. They are *polychromatic* and can be written as (5.3), integrated over k, i.e.

$$\Psi(x_1, x_2; t) = \int_0^\infty k \, dk \, \Psi^{(k)}(x_1, x_2) e^{-ikct} = \int_{\mathbb{R}^2} d^2k \, \widetilde{\Psi}(\boldsymbol{k}) e^{i(\boldsymbol{x} \cdot \boldsymbol{k} - kct)}. \tag{5.11}$$

Here $\widetilde{\Psi}(\boldsymbol{k}[k, \theta]) = \psi(k, \theta)$ is the same as in (5.2) and transforms as (5.5), but with k a 'living' *colour* parameter.

As we remarked before, the E_2 Wigner operator $\mathcal{W}^{E_2}(q, p, h)$ in (3.9) commutes with the quadratic invariant operator of the Euclidean algebra (4.5). When we form the $\mathcal{L}^2(\mathbb{R}^2)$-inner product between two *polychromatic* wavefields (5.11), their Wigner function will decompose into the integral over Helmholtz Wigner functions k,

$$W^{E_2}(\mathbf{\Phi}, \mathbf{\Psi}|q, p, h) = \int_0^\infty k\,\mathrm{d}k\,W^{(k)}(\mathbf{\Phi}^{(k)}, \mathbf{\Psi}^{(k)}|q, p, h). \tag{5.12}$$

The integral can be performed most easily over k on the last expression of (5.6), thus fixing the unirrep to $k = r/\operatorname{sinc}\frac{1}{2}\rho$; this cancels the measure (5.8), and we obtain the Euclidean Wigner function of the polychromatic model in the form

$$W^{E_2}(\mathbf{\Phi}, \mathbf{\Psi}|q, \mathbf{r}[r, \alpha]) = 4\pi^2 \int_{-2\pi}^{2\pi} \mathrm{d}\rho\,\phi(r/\operatorname{sinc}\tfrac{1}{2}\rho, \alpha - \tfrac{1}{2}\rho)^* \mathrm{e}^{-\mathrm{i}\rho q} \psi(r/\operatorname{sinc}\tfrac{1}{2}\rho, \alpha + \tfrac{1}{2}\rho).$$

$$\tag{5.13}$$

The value of the Wigner function at the point $\mathbf{r}[r, \alpha]$ is thus expressed as a line integral in the wavenumber plane, on which it takes the prototypical form of the QM Wigner function (1.8).

6. Concluding remarks

The QM Wigner function (1.8) has been very useful to visualize processes in position-momentum phase space. Paraxial optics and acoustics are also served well by this Wigner function formalism: a linear beam can be processed by purely optical means to produce an image whose intensity is the overlap between the Wigner functions of the signal (in $\mathbb{R}$) and that of the window [11]; the Wigner function (1.8) also carries holographic information of the object beam ψ with respect to the reference beam ϕ [12] in its marginal distribution on position. The Wigner function formalism presented here describes wide-angle, 2π wavefields in two-dimensional elastic media by a Euclidean Wigner function that satisfies the desirable properties of Wigner quasiprobability distribution functions. These are: covariance, the overlap formula, and the basic sesquilinearity that provides the Schrödinger cat states with a smile function.

The Wigner operator and function [3, 4], separate clearly between the geometry given by the group, and the dynamics implicit in the model. Among the groups studied so far, the Euclidean group is of special interest: it is a contraction of the (SU(2) cover of the) rotation group, and it contracts to the Heisenberg–Weyl group in the paraxial limit; it has two non-equivalent subgroups associated with continuous and discrete models, governed by differential and difference equations, respectively. For discrete signals, in particular, the Wigner function formalism provides a new understanding of classical observables of position and momentum. For wave phenomena it yields a picture incorporating both the wavenumber (Fourier transform of the field) and the wavefield localization on the screen.

Acknowledgments

References

[1] Wigner E 1932 On the quantum correction for thermodynamic equilibrium *Phys. Rev.* **40** 749–59

    Hillery M, O'Connell R F, Scully M O and Wigner E P 1984 Distribution functions in physics: fundamentals *Phys. Rep.* **106** 121–67

    Lee H-W 1995 Theory and application of the quantum phase-space distribution functions 1995 *Phys. Rep.* **259** 147–211

[2] Wolf K B 1997 Wigner distribution function for paraxial polychromatic optics *Opt. Commun.* **132** 343–52

[3] Wolf K B, Atakishiyev N M and Chumakov S M 1997 Wigner distribution function for finite signals *Photonic Quantum Computing (SPIE Proc. 3076)* (Orlando, FL) pp 196–206

    Atakishiyev N M, Chumakov S M and Wolf K B 1998 Wigner distribution function for finite systems *Preprint* IIMAS No 52 *J. Math. Phys.* submitted

[4] Atakishiyev N M, Chumakov S M, Nieto L M and Wolf K B 1998 Wigner function on groups for various optical models *Proc. Fifth Int. Conf. on Squeezed States and Uncertainty Relations NASA (Balatonfured, Hungary, 27–31 May 1997)*

[5] See, for example, Goodman J W 1968 *Introduction to Fourier Optics* (New York: McGraw-Hill) ch 2

[6] Wolf K B 1979 *Integral Transforms in Science and Engineering* (New York: Plenum) ch 1–3

[7] Abramowitz M and Stegun I A (ed) 1964 *Handbook of Mathematical Functions* (Washington DC: National Bureau of Standards) eq 16.273

[8] Steinberg S and Wolf K B 1981 Invariant inner products on spaces of solutions of the Klein–Gordon and Helmholtz equations *J. Math. Phys.* **22** 1660–3

[9] Vilenkin N Ja and Klimyk A U 1991 *Representation of Lie Group and Special Functions* vol 1 (Dordrecht: Kluwer)

[10] Wolf K B 1989 Elements of Euclidean optics *Lie methods in optics II (Springer Lecture Notes in Physics 352)* (Heidelberg: Springer) pp 116–62

[11] Lohmann A 1980 The Wigner function and its optical production *Opt. Commun.* **42** 32–7

    Bartelt H O, Brenner K-H and Lohmann H 1980 The Wigner distribtuion function and its optical production, *Opt Comm* **32** 32–38,

    Bartelt H and Brenner K-H 1980 The Wigner distribution function: an alternate signal representation in optics *Israel J. Technol.* **18** 260–2

    Brenner K-H and Lohmann H 1982 Wigner distribution function display of complex 1D signals *Opt. Commun.* **42** 310–14

[12] Wolf K B and Rivera A L 1997 Holographic information in the Wigner function *Opt. Commun.* **144** 36–42